Australian Journal of Basic and Applied Sciences, 4(8): 3917-3933, 2010
ISSN 1991-8178

Suppressing Friction-Induced Vibration Due To Negative Damping and Mode Coupling Effects Using Active Force Control

[1]S.M Hashemi-Dehkordi, [1]M. Mailah, [2]A.R. Abu-Bakar

[1]Department of Applied Mechanics, [2]Department of Automotive Engineering
Faculty of Mechanical Engineering, Universiti Teknologi Malaysia, Skudai, Johor, Malaysia.

Abstract: This paper serves to highlight a potential and effective active force control (AFC) based scheme to suppress friction induced vibration that is caused by the mechanisms of negative damping and mode-coupling. Two mathematical models that are based on Shin and Hoffmann schemes are first simulated and analyzed using a conventional closed loop proportional-integral-derivative (PID) controller. Later, the models were seamlessly integrated with AFC elements to develop into a two degree-of-freedom (DOF) controller that is designed to effectively reject the disturbances and consequently reduce the vibrations in both models. It is found that the integrated PID-AFC scheme is very effective in suppressing vibration compared to the pure PID controller alone as clearly demonstrated through the results presented both in time and frequency domains.

Key words: Friction induced vibration, negative damping, mode coupling, active force control

INTRODUCTION

Friction induced vibration (FIV) exists in almost all mechanical systems that are utilizing sliding surfaces such as a brake system, computer hard disks and machine tools. It may cause these mechanical systems to generate unwanted noise and vibration which lead to discomfort to clients and may deteriorate its performance. There are typically three major mechanisms that contribute to the generation of friction induced vibration namely: negative damping (Yuan, 1995; Shin *et al.,* 2004; Fosberry and Holubecki, 1961), sprag slip (Spurr, 1961; Jarvis and Mills, 1963-1964; Earles and Lee, 1976) and modal coupling (North, 1972; Liles, 1989; Akay *et al.,* 2000). Various techniques such as structural modification and control system have been implemented in the work of the previous researchers to reduce the effect of FIV. The following will explain some of the recent works that have been done for reducing FIV. Ouyang *et al.* (2009) presented structural modification approach in order to reduce vibration using complex eigenvalue analysis. They determined the latent roots of asymmetric systems represented by second order matrix differential equations and predicting the critical value of the parameter generating the asymmetry in the stiffness matrix, based on the receptance of the corresponding symmetric systems. Nakano and Maegawa (Nakano and Maegawa, 2009) introduced safety-design criteria to prevent friction-induced vibration by conducting dimensionless analysis and numerical simulation for a single-degree-of-freedom system with friction. The model considered a discontinuity between static and kinetic friction and the dependence of the kinetic friction coefficient on the relative velocity. Due to dimensionless description the number of parameters reduced from nine to five, where four of the five dimensionless parameters controlled the occurrence limit of friction-induced vibration. The occurrence-limit equation was derived on the basis of a previous study on stick–slip in the Coulomb friction model, and the discriminant inequalities were constructed with the four parameters in which they are sufficient conditions for preventing friction-induced vibration. Chatterjee and Mahata (Chatterjee and Mahata, 2009) employed an active absorber based on the time-delayed displacement difference feedback in controlling friction-driven vibrations. The local stability analysis shows that the static equilibrium can be locally stabilized by suitably selecting the control gain and the time-delay. The regions of stability are delineated in the plane of the control parameters. Numerical simulations of the system show that proper selections of the control parameters can also achieve the global stability of the system. As mentioned before, FIV is one of the major reasons that give a cause to disk brake noise, and it is so important that as noted by Abendroth and Wernitz (Abendroth and Wernitz, 2000), a large number of manufacturers of brake pad materials spend up to 50% of their engineering costs on issues related to noise, vibration and harshness. Brake noise vibration phenomena are described by a number of terminologies that are

Corresponding Author: M. Mailah, Department of Applied Mechanics,
Email: musa@fkm.utm.my.

sometimes interchangeably used such as squeal, groan, chatter, judder, moan and hum (Kinkaid *et al.,* 2003). Apart from those mechanisms, moving load (Mottershead *et al.,* 1997; Ouyang *et al.,* 1998; 1999) is another mechanism that leads to disk brake noise. A detailed explanation of these mechanisms can be found in (Kinkaid *et al.,* 2003).

Since then, problem of the noise and vibration in brake has been studied with experimental (Fosberry and Holubecki, 1961; Fieldhouse and Newcomb, 1993; 1991) analytical (Yuan, 1995; Shin *et al.,* 2004; Spurr, 1961; Jarvis and Mills, 1963-1964; Akay *et al.,* 2000) and finite element methods (Liles, 1989; Guan and Jiang, 1998; Abu-Bakar, 2005), but there is still as yet no method to suppress the entire brake noise and vibration in general and squeal in particular. Furthermore, a complete understanding on the problem has still not been achieved. Papinniemi *et al.* (2002) suggested that these are mainly due to the complexity of the mechanisms itself and competitive nature of automotive industry which limits the amount of cooperative research, i.e., published in the open literature or public domain.

In this paper, a closed loop control employing PID element with and without active force control (AFC) is presented. These controllers are integrated into two different mathematical models with each having two degrees-of-freedom and one of them is based on negative damping effect and the other is mode coupling effect. The main advantage of the AFC technique is its ability to reject disturbances that are applied to the system through appropriate manipulation of the selected parameters. Additionally, the technique requires much less computational burden and has been successfully established to be readily implemented in real-time. AFC as first proposed by Hewit and Burdess (1981) is robust and effective in controlling a robot arm. Mailah and fellow researchers (Pitowarno *et al.,* 2007; Priyandoko *et al.,* 2009; Mailah *et al.,* 2009) demonstrated the application of the technique to include many other dynamical systems with the incorporation of artificial intelligence (AI) methods.

2. Shin and Hoffmann Brake Models:

In this paper, two different friction induced vibration models considering the effect of negative damping and mode-coupling developed by Shin *et al.* (2002) and Hoffmann *et al.* (2004), respectively, are adopted. Figure 1 shows the Shin model and it has two DOFs which are connected through a sliding friction interface. The motion of the mass, m_1 may represent the tangential motion of the pad, and the second mass, m_2 may represent the in-plane motion of the disc. The normal force, N is a constant load that can be computed from pressure P multiplied by the surface area S. The dynamic friction coefficient is considered to reduce by the corresponding increase of the relative velocity as shown in Figure 2. The relative velocity in the figure consists of a constant velocity of the disk, v_0 added to the variable velocity of the disk and subtracted from the variable velocity of the pad. The friction coefficient or the slope α is known to be influential in contributing to the vibration in the system.

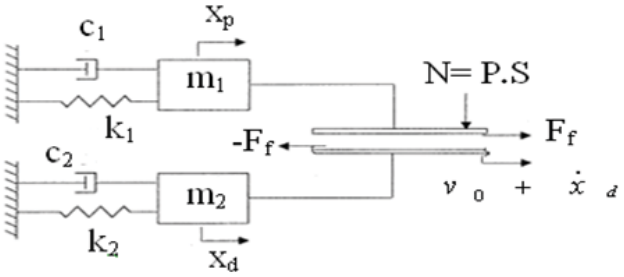

Fig. 1: Shin model of friction induced vibration

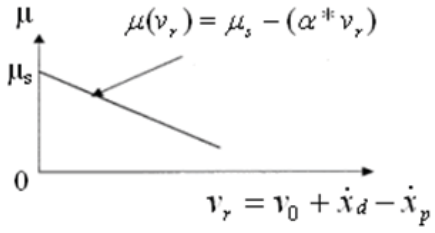

Fig. 2: Dynamic friction coefficient

Equation (1) shows the linear function of the dynamic friction coefficient:

$$\mu_k = -\alpha v_r + \mu_s \tag{1}$$

The dynamic equations of motion are written as follows (Shin *et al.,* 2002):

$$\begin{aligned} m_1\ddot{x}_p + c_1\dot{x}_p - N\alpha(\dot{x}_p - \dot{x}_d) + k_1 x_p &= N(\mu_s - \alpha v_0) \\ m_2\ddot{x}_d + c_2\dot{x}_d - N\alpha(\dot{x}_d - \dot{x}_p) + k_2 x_d &= -N(\mu_s - \alpha v_0) \end{aligned} \tag{2}$$

In order to take into account the effect of mode coupling, Hoffmann model (Hoffmann *et al.,* 2004) is adopted and is shown in Figure 3. The model has two DOFs and consists of a conveyor belt with constant velocity n_B that is pushed with a constant normal force ***N*** against a block modeled as a block of mass *m*. The model has a single-point mass sliding over a conveyor belt and there are two linear springs k_1 and k_2 parallel and normal to the belt surface with the latter regarded as the physical contact stiffness between the objects in relative sliding motion. In addition, there is another linear spring *k* mounted at oblique angle of 45° constituting the off-diagonal terms in the model's stiffness matrix. For the friction component, a coulomb model is assumed such that $F_F = m\ N$, where μ is the coefficient of kinetic friction usually taken to be constant. ***N*** is a normal force and since the normal force at the friction interface is linearly related to the vertical displacement x_2 of the mass then the resulting friction will become $F_F = m\ k_2\ x_2$.

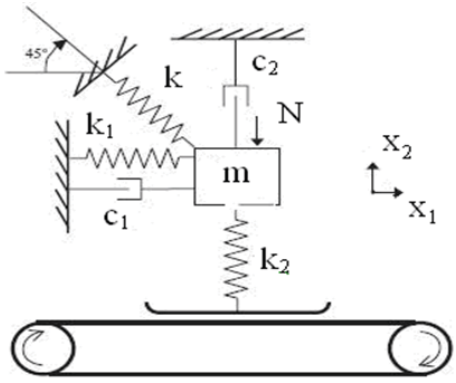

Fig. 3: Hoffmann model of friction induced vibration

The matrix form of the equation of motion can be expressed as (Hoffmann *et al.,* 2004):

$$\begin{bmatrix} m & 0 \\ 0 & m \end{bmatrix}\begin{pmatrix} \ddot{x}_1 \\ \ddot{x}_2 \end{pmatrix} + \begin{bmatrix} c_1 & 0 \\ 0 & c_2 \end{bmatrix}\begin{pmatrix} \dot{x}_1 \\ \dot{x}_2 \end{pmatrix} + \begin{bmatrix} k_1 + \frac{k}{2} & \frac{-k}{2} \\ \frac{-k}{2} & k_2 + \frac{k}{2} \end{bmatrix}\begin{pmatrix} x_1 \\ x_2 \end{pmatrix} = \begin{pmatrix} -\mu k_2 x_2 \operatorname{sgn}\left(v_B - \dot{x}_1\right) \\ N \end{pmatrix} \tag{3}$$

3. Vibration Control:

3.1 Scheme A: Suppressing Vibration Due to Negative Damping:

Having found a suitable mathematical model that represents the effect of negative damping as shown in Figure 1, it is necessary to control the vibration in both directions x_p and x_d using actuators which can apply forces that are parallel to the given axes. Thus the equations of motion having introduced the actuators can be obtained as follows:

$$m_1\ddot{x}_p + c_1\dot{x}_p - N\alpha(\dot{x}_p - \dot{x}_d) + k_1 x_p = N(\mu_s - \alpha v_0) + A_p$$
$$m_2\ddot{x}_d + c_2\dot{x}_d - N\alpha(\dot{x}_d - \dot{x}_p) + k_2 x_d = -N(\mu_s - \alpha v_0) + A_d \quad (4)$$

Where forces A_p and A_d are the actuator forces that are applied to the mathematical model.

The control strategy that is proposed here employs an AFC-based scheme that is used in conjunction with the conventional PID controller. The PID controller was first tuned with *Ziegler-Nichol's* method and then manipulated for fine performance. After wards, the AFC part is included into the system to supply the compensation of the disturbances that are inherent in the brake system. Figure 4 shows the AFC scheme applied to a dynamic translation system of the adopted models. AFC scheme is shown to be effective in providing the actuated force and body acceleration are precisely measured and at the same time the estimated mass suitably approximated (Mailah, 1998; 2000). The essential AFC equation can be related to the computation of the estimated disturbance force, F_d as follows:

$$F_d = F - M'.a \quad (5)$$

where F is the measured actuating force, M' is the estimated mass and a is the measured linear acceleration. This parameter is then fed back through a suitable inverse transfer function of the actuator to be summed up with the PID control signal. The theoretical analysis with the stability of the proposed AFC method has been described in (Burdess and Hewit, 1986). A number of methods to estimate the mass have been proposed in the previous studies such as artificial intelligence (AI) and crude approximation techniques (Mailah, 1998; 2000; Burdess and Hewit, 1986). In this study, the use of crude approximation method to approximate the estimated mass is seen sufficient. The main challenge of the AFC method is to acquire suitable estimation of the mass required to compute the disturbance F_d in the feedback loop. A conventional PID that is used with the AFC scheme can be typically represented by the following equation:

$$G_c(s) = K_p + \frac{K_i}{s} + K_d s \quad (6)$$

Where K_p, K_i and K_d are the proportional, integral and derivative gains respectively.

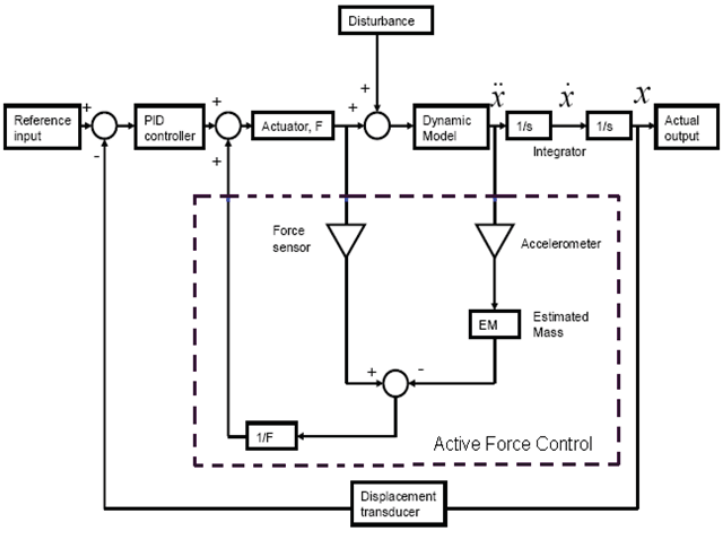

Fig. 4: Schematic diagram of AFC scheme

3.1.1 Simulation for Scheme A:

To simulate the Shin model with the controllers, MATLAB, Simulink and Control System Toolbox (CST) software are utilised. The actuators are assumed to be of linear type with a suitable constant gain. They provide the necessary external energy to suppress vibration in the model. The parameters used in this study were mostly taken from the previous research(Shin *et al.,* 2002; Hoffmann *et al.,* 2004; Utz von Wagner *et al.,*

2007; Ouyang, 2009). Nevertheless, some of them needed to be manipulated to suit the application in the simulation, and the detailed parameters are given as follows:
Mathematical model parameters:

- Body masses, m_1 = 0.2 kg, m_2=1 kg
- Spring stiffness, k_1 = 26000 N/m, k_2 = 38000 N/m
- Damping coefficient, c_1 = 2 Ns/m, c_2 = 3.5 Ns/m
- Static friction coefficient, μ_s = 0.6
- Normal preload, N = 100 N

Actuators:

- Actuators gain, Q = 0.5

Reference value:

- Reference input = 0.00 m (i.e. no vibration)

In the simulation process, several types of operating conditions are deliberately introduced to the mathematical model to evaluate the effectiveness and robustness of the control system. The Simulink diagram of the Shin model is shown in Figure 5 in which the schematic block diagram was constructed from Equation (2).

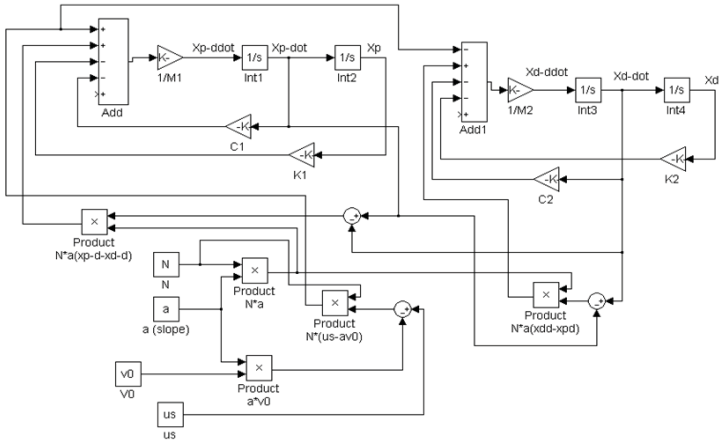

Fig. 5: Simulink diagram of Shin model

Two actuator forces for compensating the disturbances that are actually inherent in the two DOFs Shin model brake system are required. The actuator forces are controlled by two individual PID controllers involving two negative feedback loops. Thus, there are two inputs to the model that are related to the actuator forces as shown in Figure 6.

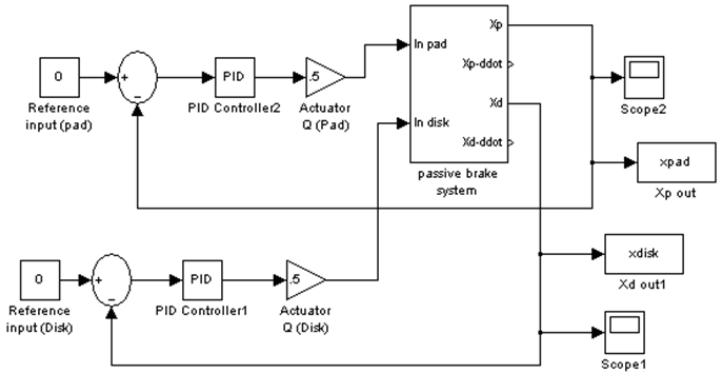

Fig. 6: Simulink diagram of the PID controller

For better vibration performance, AFC is integrated into the pure PID controller. The AFC Simulink diagram includes the estimated mass, EM and the parameter, *1/Q*. The input to the AFC is the mass

acceleration and the output is summed with the PID controller output and then multiplied with the actuator gain which subsequently generates the actuator force. To obtain the effective results, it is required to acquire a suitable estimated mass combined with appropriate tuning of the PID controller gains. Figure 7 shows an AFC scheme used in the study to suppress vibration and it can be seen that each PID controller is added to the AFC loop.

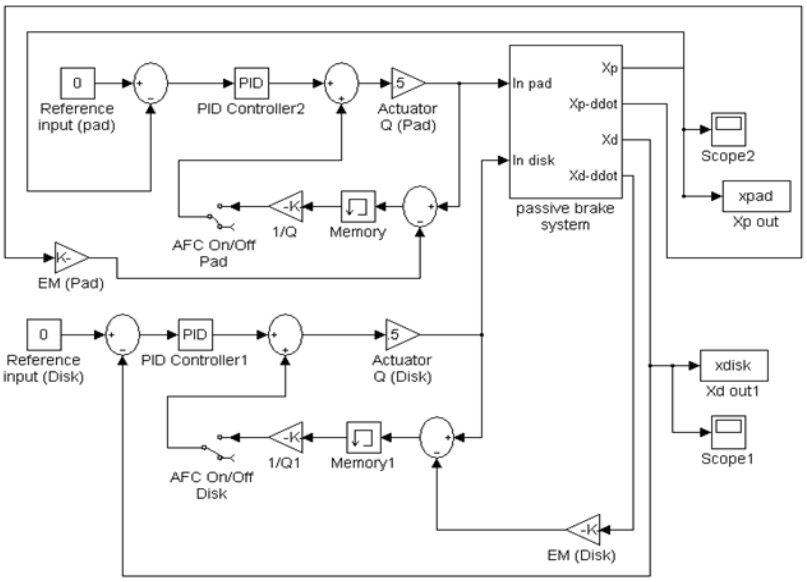

Fig. 7: Simulink diagram of the proposed AFC model

In order to tune the PID controllers, *Ziegler-Nichol*'s method is used and the results are tabulated as shown in Table 1.

Table 1: PID parameters tuned using *Ziegler-Nichol*'s method

PID	K_p	K_i	K_d
Gain	0.042	0.024	0.091

The estimated masses for the AFC loops are obtained by crude approximation method in which the appropriate value is found to be 1.2 kg and the percentage of AFC used is 100% (switch: ON), implying that the AFC loop employs full AFC implementation.

3.2 Control Scheme B: Suppressing Vibration due to Mode Coupling:

By acquiring the mathematical model that takes into account the effect of mode coupling as shown in Figure 3, it is necessary to control the vibration of the mass in vertical direction, x_2 and horizontal direction x_1. By attaching two actuators to the mass in the direction of x_1 and x_2, the controlling forces are applied directly to the system. Thus, the equation of motion is expressed as follows:

$$\begin{bmatrix} m & 0 \\ 0 & m \end{bmatrix}\begin{pmatrix} \ddot{x}_1 \\ \ddot{x}_2 \end{pmatrix}+\begin{bmatrix} c_1 & 0 \\ 0 & c_2 \end{bmatrix}\begin{pmatrix} \dot{x}_1 \\ \dot{x}_2 \end{pmatrix}+\begin{bmatrix} k_1+\frac{k}{2} & \frac{-k}{2} \\ \frac{-k}{2} & k_2+\frac{k}{2} \end{bmatrix}\begin{pmatrix} x_1 \\ x_2 \end{pmatrix} = \begin{pmatrix} -\mu k_2 x_2 \operatorname{sgn}\left(v_B-\dot{x}_1\right)+A_1 \\ N+A_2 \end{pmatrix} \tag{5}$$

where, A_1 and A_2 are the forces of the actuators that are applied to the mass. The control strategy that is used to reduce the vibration caused by mode coupling is the similar to the one explained in Section 3.1.

3.2.1 Simulation for Scheme B:

Similar to Section 3.1, MATLAB, Simulink and Control System Toolbox (CST) software were used to simulate the Hoffmann model with the controllers. The actuators were assumed to be of linear type with a suitable constant gain. The parameters used in this study are mostly taken from the work of [28]-[29], [33], [34] with the required manipulations. The detailed parameters are as follows:

Mathematical model parameters:

- Body mass, m = 0.25 kg,
- Spring stiffness, k = 15000 N/m, k_1 = 26250 N/m, k_2 = 27000 N/m
- Damping coefficient, c_1 =1.49 Ns/m, c_2 = 1.5 Ns/m
- Initial friction coefficient, μ = 0.3
- Normal pre-load, N =100 N
- Velocity of the belt, v_B=33.333 m/s =120 km/h

Actuator:

- Actuator gain, Q_1 = 3, Q_2 = 1.5

Reference value:

- Reference input = 0.0 m (i.e., no vibration)

The Simulink diagram of the Hoffmann model constructed from Equation (3) is shown in Figure 8.

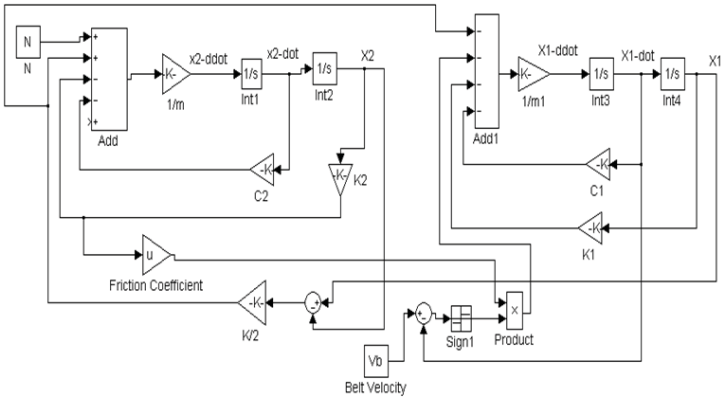

Fig. 8: Simulink diagram of the Hoffmann model

Having developed a Simulink diagram for the Hoffmann model, the PID controller is integrated into the Hoffmann model by installing two actuators which provide the controlling forces for compensating and reducing the vibrations that occur in x_1 and x_2 directions where actuator forces are controlled by two PID controllers which typically involve two negative feedback loops. There are two inputs to the PID controller which correspond to the two actuator forces as shown in Figure 9.

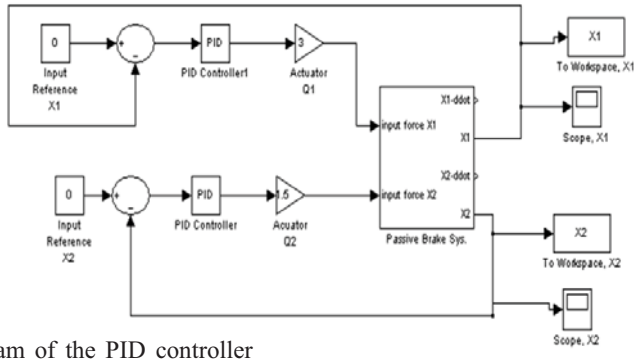

Fig. 9: Simulink diagram of the PID controller

For achieving better vibration performance in the Hoffmann model, the AFC is fully integrated with the PID controller. For better predictive results, it is required to have a suitable mass estimation combined with the best tuning of the PID controller gains. Figure 10 shows a Simulink diagram of the proposed AFC controller.

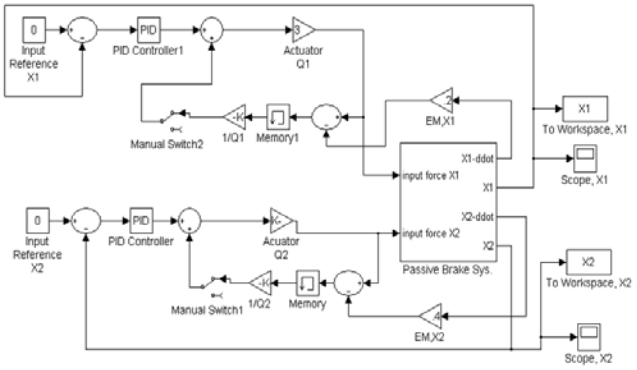

Fig. 10: Simulink diagram of the proposed AFC controller

Table 2 shows the values of the estimated mass and the PID parameters in which they mere mainly obtained by trial and error or crude approximation method. Also, the percentage of the AFC used is 100% (switch is set to ON).

Table 2: The values for the estimated mass and the PID parameters

PID Parameters	K_p	K_i	K_d
PID x_1	3.5	1.5	6
PID x_2	0.5	0.02	0.08
Estimated Mass (kg)			
EM x_1	0.2		
EM x_2	0.4		

RESULTS AND DISCUSSION

4.1 Scheme A: Effect of Negative Damping:

First, the slop α in the equation of dynamic friction coefficient is set to 0.015 (negative damping) and with a constant velocity of 90 km/h where simulation is initially performed using only the pure PID controller. The results of this process can be seen in Figures 11 (a) and (b). It can be noticed that the vibration that may result in producing noise is quite high mainly in the first 2 seconds nevertheless it converges to a steady state condition towards the end of the simulation period. Later on, the simulation is carried out again but this time considering 100% AFC mode plus the PID controller. Contrary to the previous scheme, the vibration almost disappeared instantaneously and the system seems to operate very smoothly throughout the simulation period.

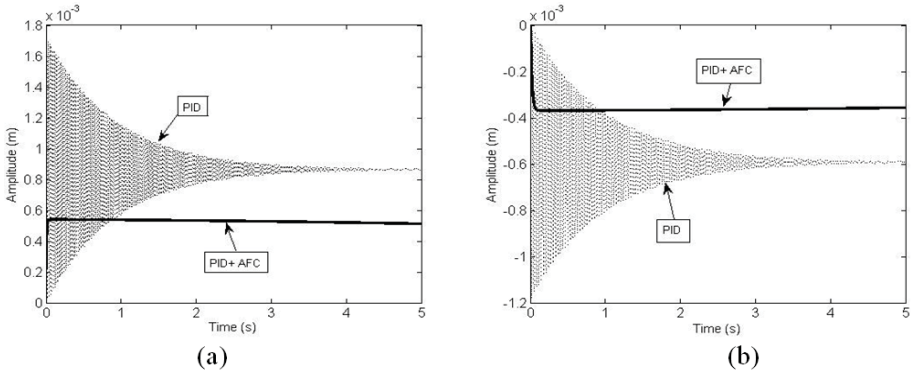

Fig. 11: Vibration response in the direction of (a) x_p with $\alpha = 0.015, v_0 = 90km/h$ (b) x_d with $\alpha = 0.015, v_0 = 90km/h$

During the next simulation test, the slope with negative damping is increased to 0.02 with the same constant velocity; the results of this simulation are shown in Figures 12 (a) and (b).

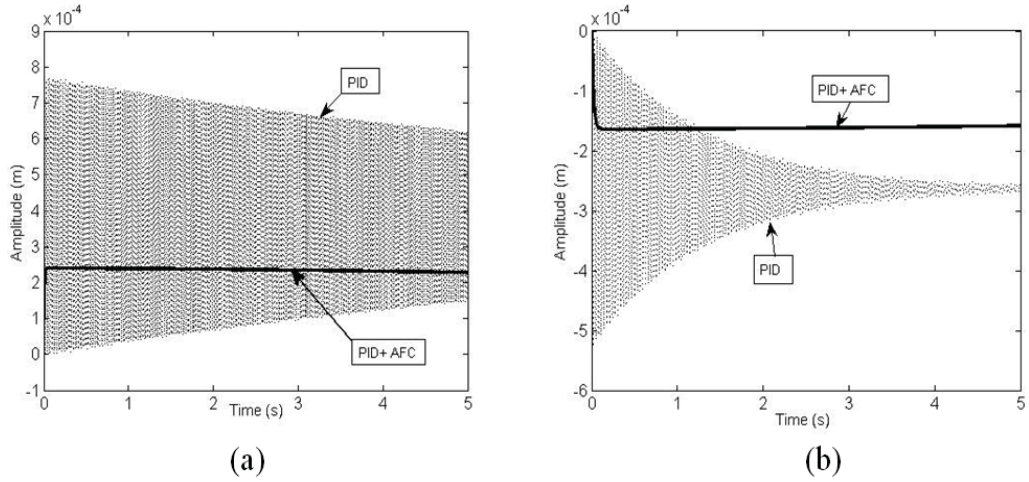

Fig. 12: Vibration response in the direction of (a) x_p with $\alpha = 0.02, v_0 = 90km/h$

(b) x_d with $\alpha = 0.02, v_0 = 90km/h$

It can be seen that with a pure PID controller, the vibration of the pad (m_1) is not reduced notably though the trend is converging, but when the mode is switched to AFC with the PID scheme, the vibrations are again very much reduced to a steady state condition almost immediately. The frequency response analyses are also carried out and the results are shown in Figures 13 (a) and (b) and Figures 14 (a) and (b). It can be seen that the PID controllers obviously produce considerable sharp spikes with high amplitude at around 50 Hz and 30 Hz while the AFC-based schemes hardly produces any peaks, thus verifying the effectiveness of the system performance.

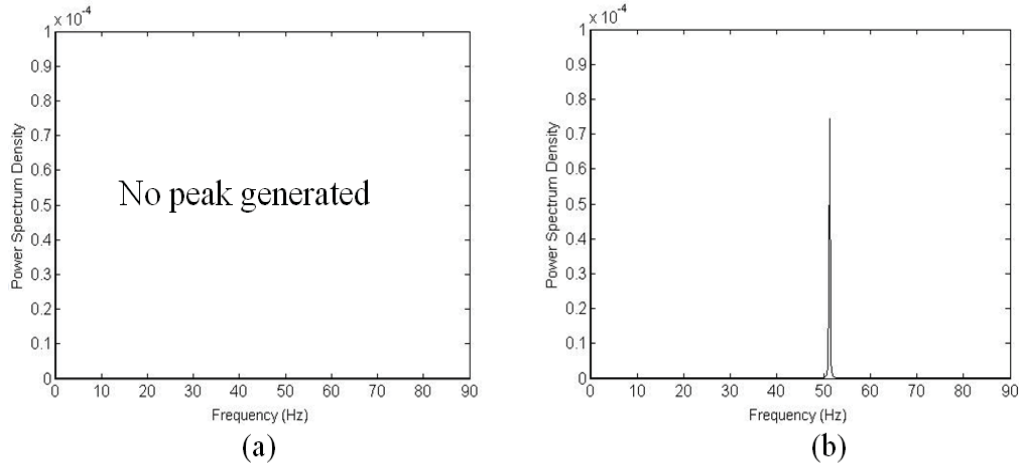

Fig. 13: Results in frequency domain in the direction of x_p with $\alpha = 0.02, v_0 = 90km/h$ for (a) PID+AFC (b) PID schemes

When the slope of negative damping is set to 0.025, it can be seen in Figures 15 and 16 that the system can no longer be stabilized with a PID controller as the vibrations are increasing in amplitude with the increase in time. In contrast, after applying AFC to the PID controller, the vibrations in the system are considerably and consistently reduced to nearly zero level. The frequency response of this simulation procedure is shown in Figures 17 and 18.

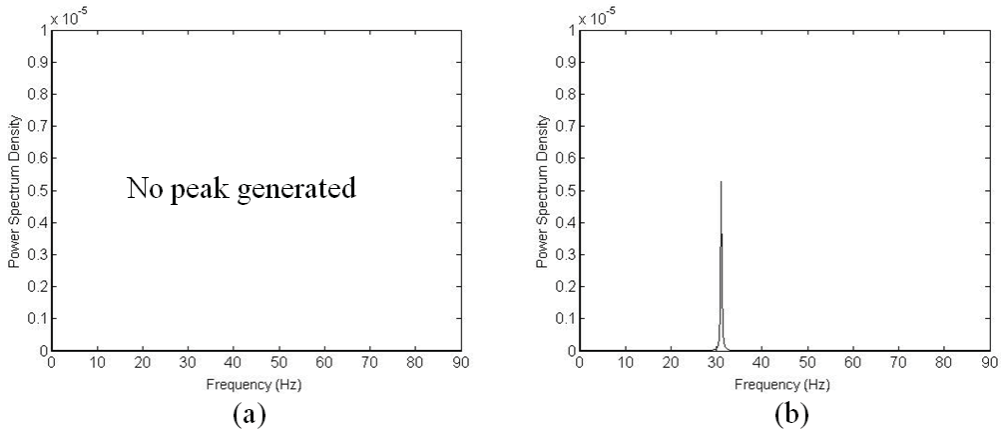

Fig. 14: Results in frequency domain in the direction of x_d with $\alpha = 0.02, v_0 = 90km/h$ for (a) PID+AFC (b) PID schemes

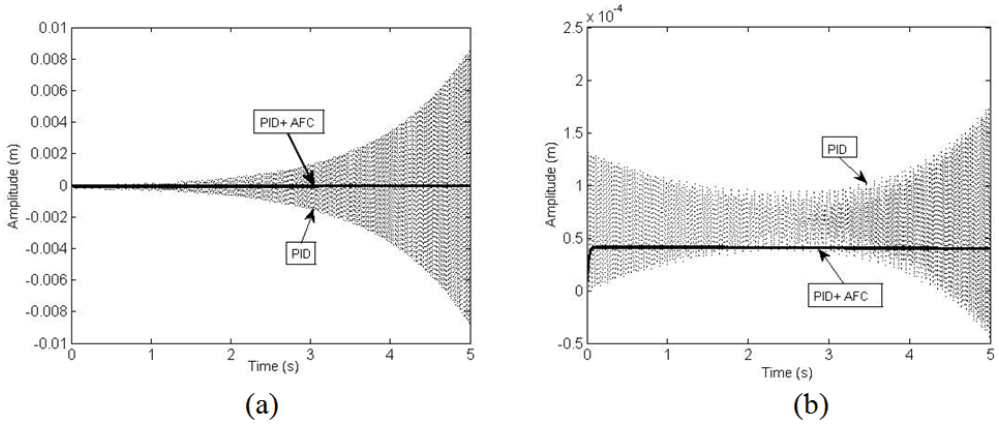

Fig. 15: Vibration response in the direction of (a) x_p with $\alpha = 0.025, v_0 = 90km/h$

(b) x_d with $\alpha = 0.025, v_0 = 90km/h$

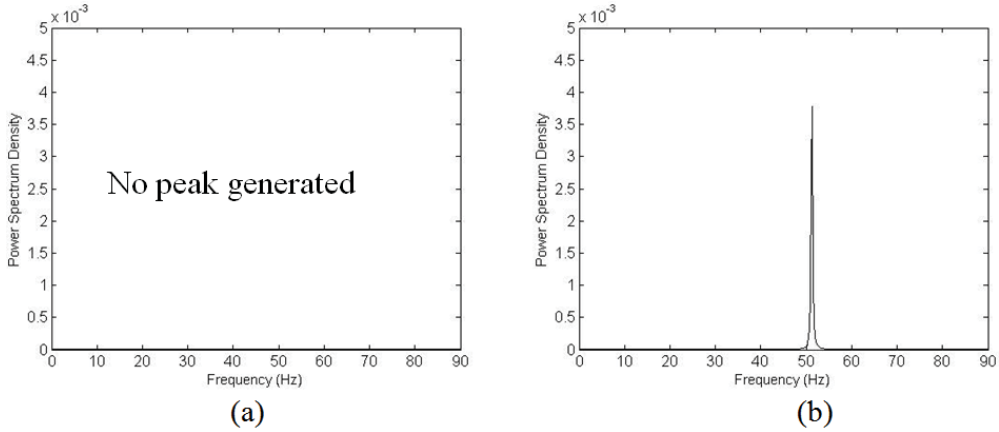

Fig. 16: Results in frequency domain in the direction of x_p with $\alpha = 0.025, v_0 = 90km/h$ for (a) PID+AFC (b) PID schemes

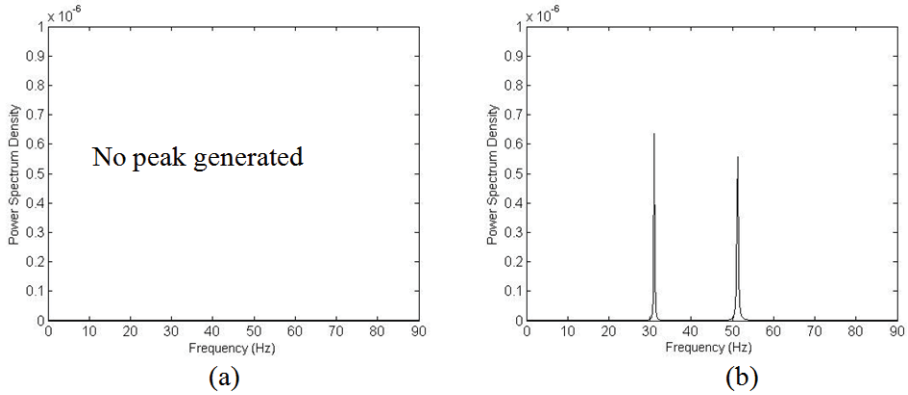

Fig. 17: Results in frequency domain in the direction of x_d with $\alpha = 0.025, v_0 = 90km/h$ for (a) PID+AFC (b) PID schemes

In this paper, the effect of negative damping at low speed is also taken into consideration, by running the simulation under a constant velocity of 25 km/h and keeping the slope with negative damping to 0.025. Figures 18 (a) and (b) show the results of this simulation. Vibrations in the system are shown to have increased significantly in magnitude compared to the case where the speed is set at 90km/h. Therefore, it can be safely deduced that the negative damping has more adverse effect on the system at low speed. Again, when AFC is integrated with the PID controller, the result is as predicted in which the vibrations are very much suppressed. Figurers 19 (a) and (b) and Figures 20 (a) and (b) show the frequency responses of this simulation.

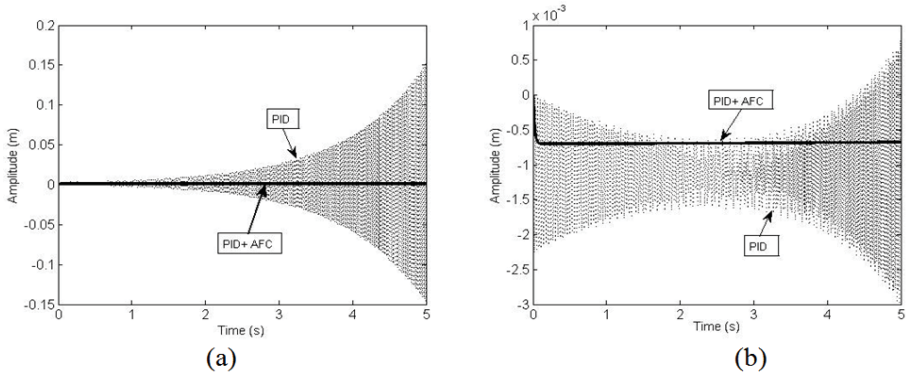

Fig. 18: Vibration response in the direction of (a) x_p with $\alpha = 0.025, v_0 = 25km/h$ (b) x_d with $\alpha = 0.025, v_0 = 25km/h$

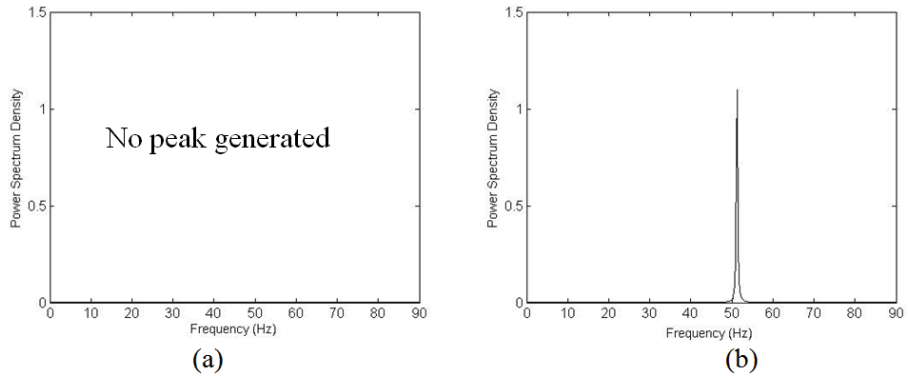

Fig. 19: Results in frequency domain in the direction of x_p with $\alpha = 0.025, v_0 = 25km/h$ for (a) PID+AFC (b) PID schemes

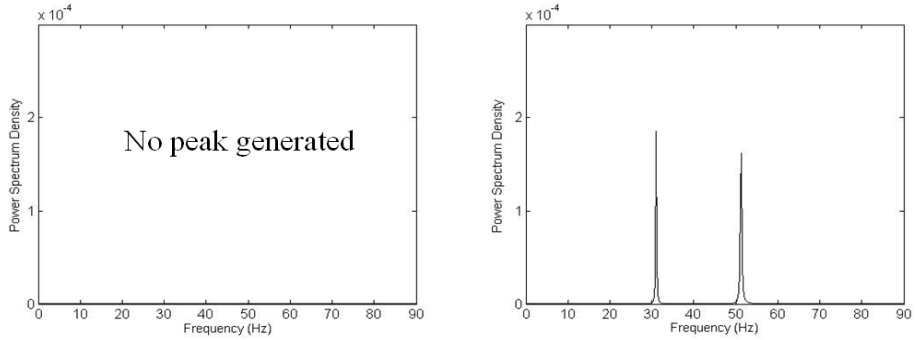

Fig. 20: Results in frequency domain in the direction of x_d with $\alpha = 0.025, v_0 = 25km/h$ for (a) PID+AFC (b) PID schemes

4.2 Scheme B: Effect of Mode Coupling:

At first, the simulation is run under normal condition, in which the initial coefficient of friction was, m = 0.3. The simulation is performed without using AFC and only the pure PID controller is applied. The result of this simulation can be seen in Figures 21 (a) and (b). It is shown that the vibration level in both directions is relatively high, but when the simulation is carried out with considering the PID controller plus 100% AFC engaged (switched on), significant reduction in vibration is observed.

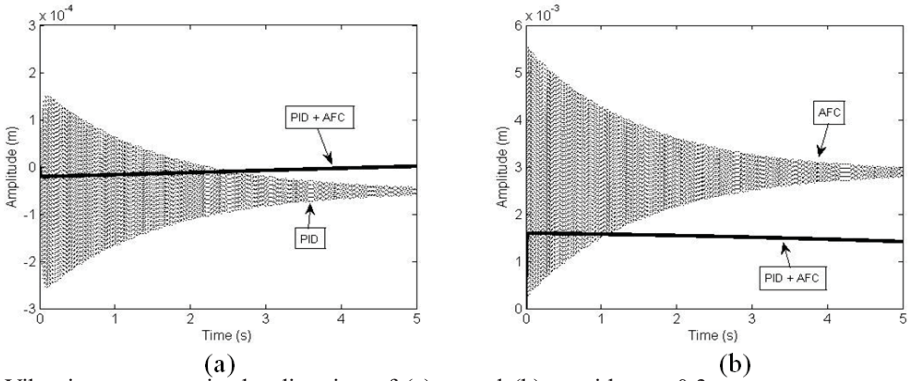

Fig. 21: Vibration response in the direction of (a) x_1 and (b) x_2 with μ = 0.3

Responses in the frequency domain are also obtained in directions x_1 and x_2 as shown in Figures 22 (a) and (b) and 23 (a) and (b), respectively.

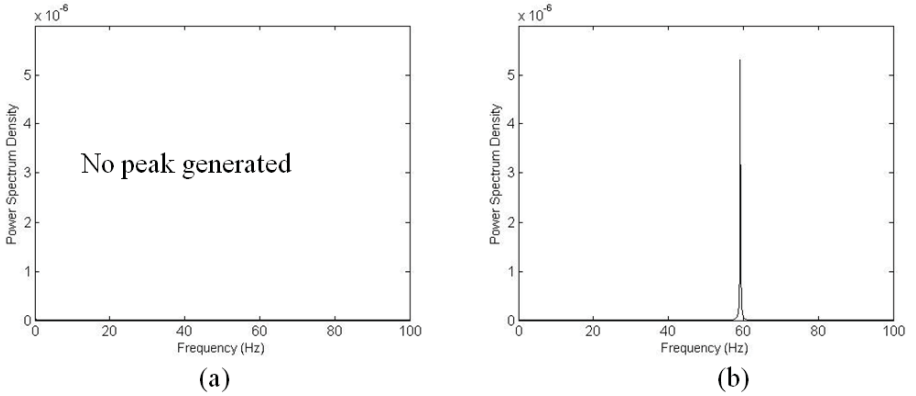

Fig. 22: Results in frequency domain in the direction of x_1 with μ = 0.3 for (a) PID+AFC (b) PID schemes

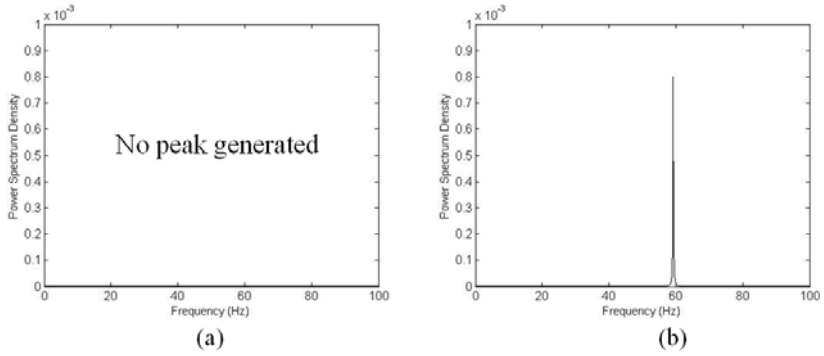

Fig. 23: Results in frequency domain in the direction of x_2 with μ = 0.3 for (a) PID+AFC (b) PID schemes

The second simulation was performed with the friction coefficient equals 0.303. It can be seen in Figures 24 (a) and (b) that the trends of the results are similar to the previous cases but with a notable increase in the magnitudes of the vibration. The PID controllers are less effective in reducing the vibrations. On the other hand, after applying AFC to the PID controller, the vibration level is largely reduced.

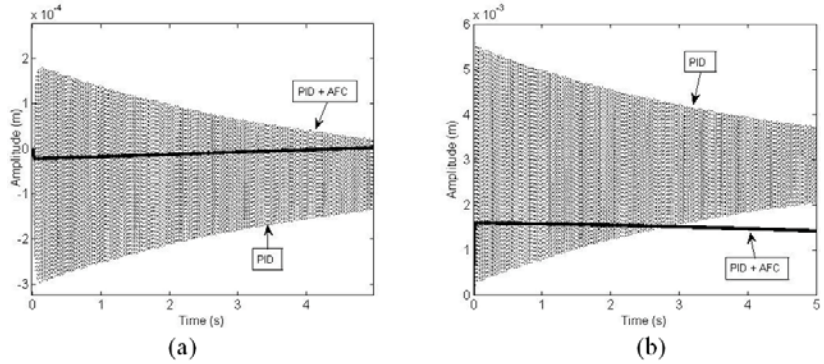

Fig. 24: Vibration response in the direction of (a) x_1 and (b) x_2 with μ = 0.303

It can be noticed from the results that when the value of the friction coefficient is: m = 0.3, the system is stable because it readily converges with time. Conversely, when the friction coefficient is increased to a certain value the responses of the system became unstable. The minimum value of m that makes the system unstable is known as the *critical friction coefficient,* m_{cr}. By trial and error or crude approximation, we found that this value is 0.305. Figures 25 (a) and (b) shows the responses of the system when m_{cr} is applied to it. It can be observed that when the system has only a PID controller, the response is very unstable and the vibration swiftly increases with time, meaning unstable system.

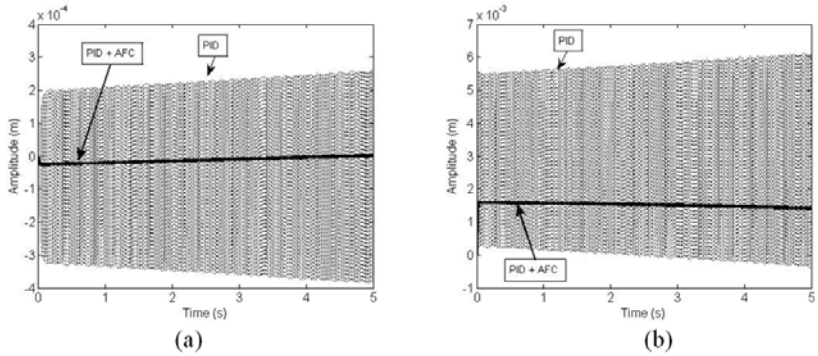

Fig. 25: Vibration response in the direction of (a) x_1 and (b) x_2 with μ = 0.305

However, the stability of the system is considerably improved when the PID controller is integrated with AFC element as shown in Figure 25. The results in frequency domain are shown in Figures 26 and 27.

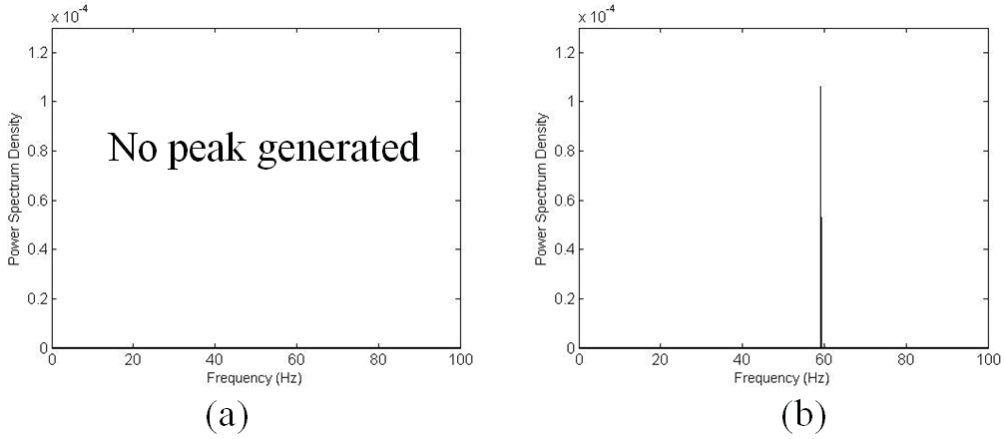

Fig. 26: Frequency domain in the direction of x_1 with μ = 0.305 for (a) PID+AFC (b) PID schemes

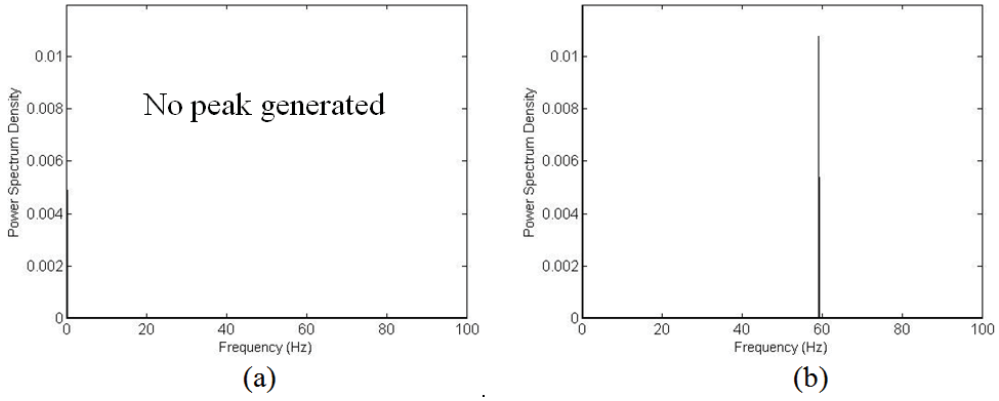

Fig. 27: Frequency domain in the direction of x_2 with μ = 0.305 for (a) PID+AFC (b) PID schemes

After finding the critical friction coefficient, the last two simulations are to increase the friction coefficient to 0.307 and 0.35. Then by running the simulations, it is noticed by the results in Figures 28 and 29 that the vibrations have got very unstable and the PID controller is unable to suppress the vibrations. However, after engaging AFC to the PID controller the vibrations in the system reduced very much.

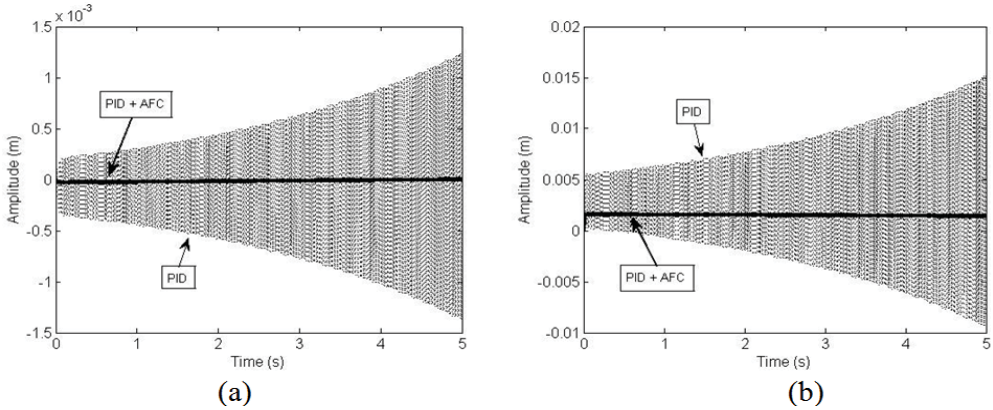

Fig. 28: Vibration response in the direction of (a) x_1 and (b) x_2 with μ = 0.307

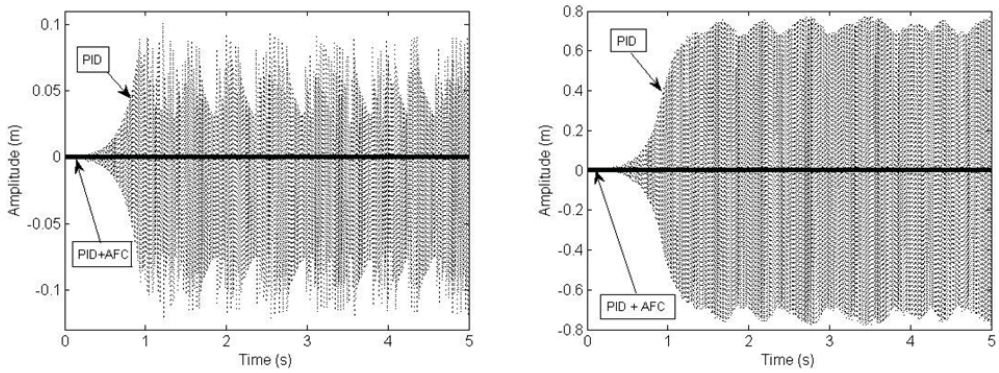

Fig. 29: Vibration response in the direction of (a) x_1 and (b) x_2 with μ = 0.35

The frequency response of the brake model operating with a friction coefficient of 0.35 is shown in Figures 30 and 31.

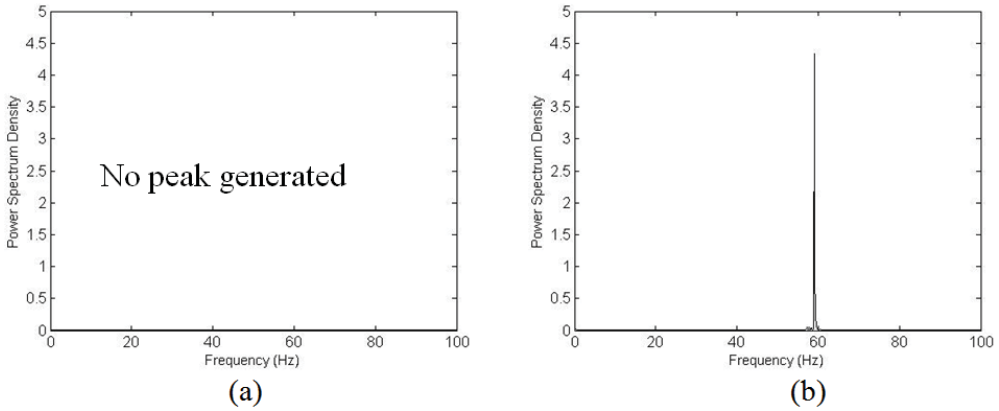

Fig. 30: Results in frequency domain in the direction of x_1 with μ = 0.35 for (a) PID+AFC (b) PID schemes

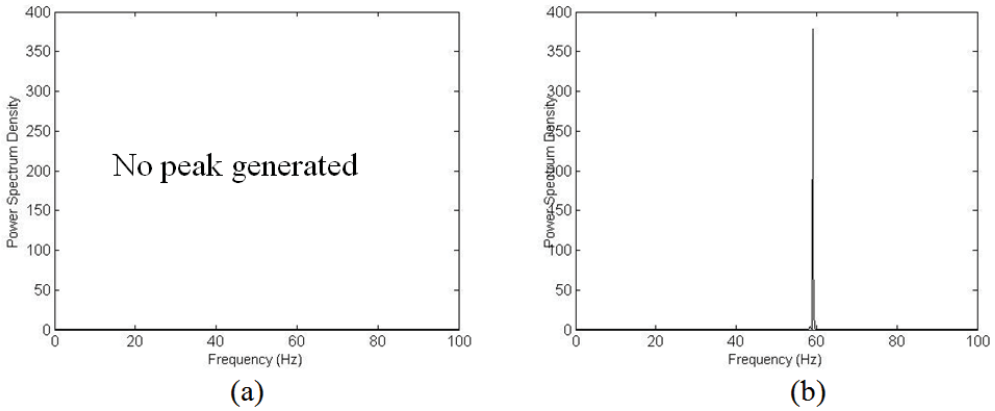

Fig. 31: Results in frequency domain in the direction of x_2 with μ = 0.35 for (a) PID+AFC (b) PID schemes

Conclusion:

An active force control based method has been developed and implemented to significantly reduce the friction induced vibration due to the effects of negative damping and mode coupling. The AFC component is readily incorporated into a PID controller and the resulting two DOF scheme has been shown to be very effectively in suppressing the vibration of both the Shin and Hoffmann models for a number of different

operating conditions. It was observed that in some cases, a pure PID controller alone is able to reduce the vibration but more often than not, it is much less effective compared to the PID plus AFC scheme in the presence of disturbances.

With the increase in friction coefficient in mode coupling or the slope of the linear friction coefficient in negative damping, a pure PID controller was unable to stabilize the system and the vibration was shown to gradually increase in amplitude with time. However, when the AFC mode is activated, the vibration was very much reduced, thereby rendering the system very stable and robust. The effect of negative damping is more severe when the system is operating at low speed. Future works may include the development of an experimental rig to verify the theoretical concept.

REFERENCES

Abendroth, H. and B. Wernitz, 2000. The Integrated Test Concept: Dyno-vehicle, Performance-noise, Technical Report 2000-01-2774, SAE, Warrendale, PA.

Abu-Bakar, A.R., 2005. Modeling and Simulation of Disc Brake Contact Analysis and Squeal, PhD Thesis, Department of Engineering, University of Liverpool, UK.

Akay, A., J. Wickert and Z. Xu, 2000. Investigating Mode Lock-in and Friction Interface, Final Research Report, Carnegie Mellon University, 1-52.

Burdess, J.S., J.R. Hewit, 1986. An active method for the control of mechanical systems in the presence of unmeasurable forcing Mechanism and Machine Theory, 21(5): 393-400.

Chatterjee, S. and P. Mahata, 2009. Time-delayed absorber for controlling friction-driven vibration, Journal of Sound and Vibration, 322: 39-59.

Earles, S.W.E. and C.K. Lee, 1976. Instability Arising from the Friction Interaction of a Pin-Disc System Resulting in Noise Generation, ASME Journal of Engineering for Industry, 98: 81-86.

Fieldhouse, J.D. and P. Newcomb, 1993. The Application of Holographic Interferometry to the Study of Disc Brake Noise, S.A.E. Technical Paper 930805.

Fieldhouse J.D. and T.P. Newcomb, 1991. An Investigation into Disc Brake Noise using Holographic Interferometry, IMechE, C427/11/213.

Fosberry, R.A. and Z. Holubecki, 1961. Disc Brake Squeal: Its Mechanism and Suppression, M.I.R.A. Technical Report.

Guan, D. and D. Jiang, A Study, 1998. on Disc Brake Squeal using Finite Element Methods, S.A.E. Technical Paper 980597.

Hewit, J.R. and J.S. Burdess, 1981. Fast Dynamic Decoupled Control for Robotics using Active Force Control, Mechanisms and Machine Theory, 16(5): 535-542.

Hoffmann, N., S. Bieser and L. Gaul, 2004. Harmonic balance and averaging techniques for stick-slip limit-cycle determination in mode-coupling friction self-excited systems, Technische Mechanik 24:185.

Huajiang Ouyang, Luis Baeza and Shaolin Hu, 2009. A receptance-based method for predicting latent roots and critical points in friction-induced vibration problems of asymmetric systems, Journal of Sound and Vibration, 321: 1058-1068.

Jarvis, R.P. and B. Mills, 1964. Vibration Induced by Dry Friction, Procs. of the Institution of Mechanical Engineers, 178: 847-866.

Kinkaid, N.M., O.M. O'Reilly and P. Papadopoulos, 2003. Review: Automotive Disc Brake Squeal, Journal of Sound and Vibration, 267: 105-166.

Liles, G.D., 1989. Analysis of Disc Brake Squeal Using Finite Element Methods. SAE Paper 891150.

Mottershead, J.E., H. Ouyang, M.P. Cartmell and M. I.Friswell, 1997. Parametric Resonances in An Annular Disc, with A Rotating System of Distributed Mass and Elasticity; and the Effects of Friction and Damping. Proceedings of the Royal Society of London A, 453(1): 1-19.

Mailah, M., H. Jahanabadi, M.Z.M. Zain, G. Priyandoko, 2009. Modelling and Control of Human-Like Arm using Active Force Control, Proc. of IMechE Part C: Journal of Mechanical Engineering Science, 223(7): 1569-1577.

Mailah, M., 1998. Intelligent active force control of a rigid robot arm using neural network and iterative learning algorithms, Ph.D Thesis, University of Dundee, UK.

Mailah, M. and N.I.A. Rahim, 2000. Intelligent active force control of a robot arm using fuzzy logic, in: Proceedings of IEEE International Conference on Intelligent Systems and Technologies, Kuala Lumpur, Malaysia, 2: 291-296.

Nakano, K. and S. Maegawa, 2009. Safety-design criteria of sliding systems for preventing friction-induced vibration, Journal of Sound and Vibration doi:10.1016/j.jsv.2009.02.027

North, M.R., 1972. Disc Brake Squeal – A Theoretical Model, Tech. Report.

Ouyang, H., J.E. Mottershead, M.P.Cartmell and M.I. Friswell, 1998. Friction-induced Parametric Resonances in Discs: Effect of A Negative Friction-velocity Relationship, Journal of Sound and Vibration, 209(2): 251-264.

Ouyang, H., J.E. Mottershead, D.J. Brookfield, S. James, M. P. Cartmell, T. Kaster, T. Treyde, B. Hirst, and R. Allen, 1999. Dynamic Instabilities In A Simple Model of A Car Disc Brake, SAE paper 1999-01-3409.

Ouyang, H., 2009. Prediction and assignment of latent roots of damped asymmetric systems by structural modifications, Mechanical Systems and Signal Processing, 23: 1920–1930.

Papinniemi, A., Lai, J.C.S., Zhao, J. and L. Loader, 2002. Brake Squeal: A Literature Review, Applied Acoustics, 63: 391-400.

Pitowarno, E. and M. Mailah, 2007. Control of Mobile Manipulator Using Resolved Acceleration Iterative Learning Proportional-Integral Active Force Control, International Review of Mechanical Engineering, 1(5): 549-558.

Priyandoko, G., M. Mailah and H. Jamaluddin, 2009. Vehicle Active Suspension System using Skyhook Adaptive Neuro Active Force Control, Mechanical Systems and Signal Processing, 23(3): 855-868.

Shin, K., M.J. Brennan, Y-G. Joe and J-E. Oh, 2004. Simple Models to Investigate the Effect of Velocity Dependent Friction on the Disk Brake Squeal Noise, International Journal of Automotive Technology, 5(1): 61-67.

Shin, K., M.J. Brennan and J.-E. Oh, C.J. Harris, 2002. Analysis of Disk Brake Noise using A Two-degree-of-freedom Model, Journal of Sound and Vibration, 254(5): 837–848.

Spurr, R.T., 1961. A Theory Of Brake Squeal, Proc. Auto. Div. Instn. Mech Eng., 62(1): 33-52.

Utz von Wagner, D. Hochlenert and P. Hagedorn, 2007. Minimal Models for Disk Brake Squeal, Journal of Sound and Vibration, 302: 527-539.

Yuan, Y., 1995. A Study of the Effects of Negative Friction-Speed Slope on Brake Squeal, DE-.84-1: 1153-1162.